Silva Fennica vol. 55 no. 1 article id 10444
Category: research article
https://doi.org/10.14214/sf.10444
http://www.silvafennica.fi
ISSN-L 0037-5330 | ISSN 2242-4075 (Online)
The Finnish Society of Forest Science

Risto Kalliola, Timo Saarinen and Niko Tanski

Seasonal variations of foliar element distributions of silver birch in different habitats

Kalliola R., Saarinen T., Tanski N. (2021). Seasonal variations of foliar element distributions of silver birch in different habitats. Silva Fennica vol. 55 no. 1 article id 10444. 16 p. https://doi.org/10.14214/sf.10444

Highlights

- Detailed mapping using micro X-ray fluorescence showed element variations in a seasonal cohort of silver birch leaves in six different habitats.
- Seasonal changes occurred in most of the ten studied nutrient elements.
- Different habitats showed unique seasonal development patterns in specific elements.
- Element distributions within individual leaf blades were variable.
- Phenotypic plasticity of foliar nutrients supports adaptation to patchy environments.

Abstract

Novel information on silver birch (*Betula pendula* Roth) foliar element contents and their seasonal, between-habitat and leaf level variations are provided by applying fine-scaled element mapping with micro X-ray fluorescence. In the monthly leaf samples collected from May to October from six different habitats, pairwise scatter plots and Spearman's rank correlations showed statistically significant positive correlations between Si, Al and Fe, and covariations between also many other pairs of elements. Of the ten elements studied, seven showed statistically significant changes in their average levels between May and June. The contents of P, S and K decreased in most habitats during the later season, whereas Ca and in some habitats also Mn and Zn increased. Comparing habitats, trees in the limestone habitat had relatively low content of Mg, strongly increasing levels of P until the late season, and high content of Ca and Fe. Other habitats also revealed distinctive particularities in their foliar elements, such as a high relative content of S and a low content of Ca at the seashore. Mn was high in three habitats, possibly due to bedrock characteristics. Except for P, the contents of all elements diverged between the midrib and other leaf areas. Zn content was particularly high in the leaf veins. Mn levels were highest at the leaf margins, indicating a possible sequestration mechanism for this potentially harmful element. Si may help to alleviate the metallic toxicities of Al and Fe. Because the growing season studied was dry, some trees developed symptoms of drought stress. The injured leaf parts had reduced levels of P, S and K, suggesting translocation of these nutrients before permanent damage.

Keywords *Betula pendula*; deciduous tree; drought injury; element mapping; foliar nutrients; X-ray fluorescence
Address Department of geography and geology, University of Turku, FI-20014 Turku, Finland
E-mail risto.kalliola@utu.fi
Received 16 September 2020 **Revised** 18 February 2021 **Accepted** 24 February 2021

1 Introduction

In temperate and boreal latitudes, the leaves of summergreen plants undergo a sequence of changes from bud burst and young leaf development to mature foliar canopies and senescing autumn leaves, which finally fall down. Although the adaptive significance of the genetically controlled deciduous habit is well known (Chabot and Hicks 1982), the study of element translocations during this process can lend understanding to how plants respond to their environment. Foliar diagnosis can provide information regarding tree nutrition and the chemical aspects of site quality (McHargue and Roy 1932). For example, Pavlović et al. (2017) suggest that chemicals accumulated in the leaves of horse chestnut (*Aesculum hippocastanum* L.) could be useful bioindicators of pollutants in urban soils.

Seasonal changes in foliar nutrient concentrations have been studied occasionally over the years, including, for example, selected temperate deciduous trees (*Quercus* spp., *Carya ovata* (Mill.) K.Koch and *Acer* spp.: Mitchell 1936), silver birch (*Betula pendula* Roth: Tamm 1951), four taiga trees (*Larix laricina* (Du Roi) K.Koch*, Picea mariana* (Mill.) Britton, Sterns & Poggenb.*, Betula papyrifera* Marshall and *Alnus crispa* (Aiton) Pursh: Chapin III and Kedrowski 1983), red maples (*Acer rubrum* L.: Messenger 1984), downy birch (*Betula pubescens* Ehrh.: Ferm and Markkola 1985) and Pyrenean oak (*Quercus pyrenaica* Steven: Santa Regina et al. 1997). The results of these investigations generally show high concentrations of nitrogen (N), phosphorus (P) and potassium (K) in young leaves with a decreasing trend toward the late summer, and increases of calcium (Ca), iron (Fe) and manganese (Mn) in the same time frame. Changes in concentrations of zinc (Zn), magnesium (Mg) and copper (Cu) are more variable. Also, the needles of the evergreen Scotch pine (*Pinus sylvestris* L.) reveal both seasonal variations in these elements and varying concentrations of N, P and K in consecutive years (Helmisaari 1990).

The aforementioned studies measured element concentrations from complete oven-dried leaves, with no information provided about the fine-scaled element distributions within individual leaf blades. As leaves are composed of several tissue types and perform diverse functions, finer-scale analytical methods could provide deeper insight into their foliar element dynamics. Such information can be obtained using the micro X-ray fluorescence (micro-XRF) method, which supports detailed element mapping in diverse materials (Fittschen and Falkenberg 2011). Researchers have been using this method to study plant tissues and their physiological functioning in various types of investigations into plant-soil relationships, environmental pollution and agricultural practices. Voegelin et al. (2007) recorded accumulations of Fe and arsenic (As) around plant roots in contaminated riparian floodplain soils; Tian et al. (2015) showed the enrichment of Zn within the sunflower petioles after the use of foliar fertilisers containing Zn; and Fittschen et al. (2017) took advantage of the non-destructive nature of micro-XRF and used it to study the living leaves of *Arabidopsis thaliana* (L.) Heynh. Gupta et al. (2019) combined micro-XRF with mass spectrometry platforms to yield precise information about the localization of lipids, metabolites and elements in germinating seeds. However, to our knowledge, this technique has not been used in the study of seasonal chemical changes in the leaves of deciduous trees.

We employ the micro-XRF technique to map the foliar contents of ten different elements in a seasonal cohort of silver birch (*B. pendula*) in six different habitats. Based on earlier studies (see references above), we expect seasonal changes to occur in many if not all of the nutrients studied. Comparing different habitats enables us to assess the role of permanent site properties in these changes (Fontana et al. 2018). Because the physiological functions of the different elements vary (Marschner 2012), we furthermore expect micro-XRF to provide unprecedented information about spatial changes in element distributions within individual leaf blades. Finally, because the early summer of the study year was dry, causing partial leaf drying in individual trees, we use the opportunity to examine how nutrient contents change in drought-injured parts of leaves.

2 Materials and methods

The study area in the municipality of Parainen is situated at ca. 60° N, in the innermost zone of the SW Finnish archipelago by the Baltic Sea (Fig. 1). The bedrock is dominated by metamorphic Svecofennian supracrustal rocks (Karhunen 2004) with Paleoproterozoic, amphibolite and granulite facies microcline granites, metabasalts, pelitic metasediments, metagranodiorites and marbles. The landscape comprises rockhill outcrops alternating with forests growing on predominantly shallow sandy to silty soils and valleys with silty to clayey soils. The latter-mentioned areas are often in agricultural use. The climate is hemiboreal humid continental (Dfb class) according to Köppen's classification (Peel et al. 2007). The average annual temperature is 5.5 °C, and the average annual precipitation is 723 mm. During the fieldwork year of 2018, temperatures were close to the average, but precipitation was unusually low during the early summer.

We collected foliar samples from birches growing in six different habitats. ROCKHILL (trees 1–3) refers to a granodiorite hill where bare rock alternates with scattered thin soil (mainly organic) and trees grow their roots in rock cracks. RURAL (trees 4–6) describes the transition of a countryside yard and an arable field with silty to silt-clay soils with good vegetative growth. SEASHORE (trees 7–9) refers to trees sampled on clay or clay-silt soils at a distance of less than two meters from the average shoreline of the Baltic Sea, which in this area has very low salinity (ca. 6‰, Suominen et al. 2010). ROAD MARGIN (trees 10–12) includes trees growing in the immediate vicinity of an asphalt road with high traffic (ca. 10 000 vehicles per day) with one tree (number 10) growing on a minor-sized granodiorite outcrop and the rest on silty soils. SEEPWATER (trees 13–15) is a forested site slightly downhill from an abandoned landfill with its low-lying parts covered with reddish mud, suggesting seepage of iron-rich water from the landfill. LIMESTONE (trees 16–18) refers to sites with thin soils just beside the fence of a major-sized quarry of marble-like limestone.

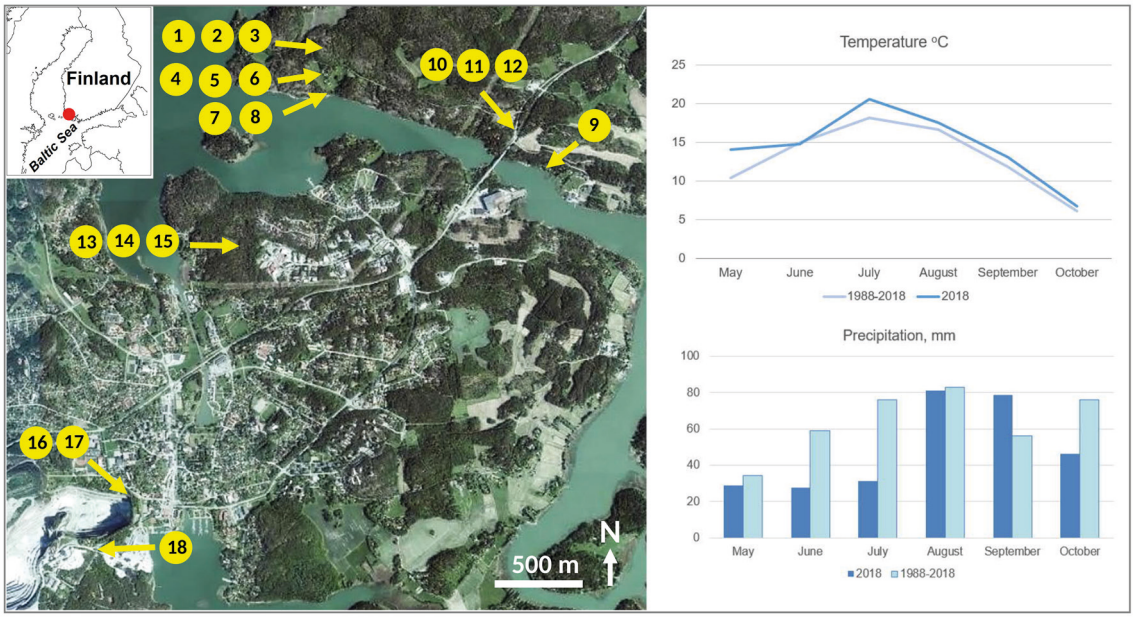

Fig. 1. Locations of the sampling points in the study area on an orthoimage showing the overall landscape structure (source: https://kartta.paikkatietoikkuna.fi/). Forests are dark green, open fields light green, and the residential areas are pale. The white area in the lower left corner is the limestone quarry. The right panel shows climatic data from the weather station Yltöinen (Kaarina) of the Finnish Meteorological Institute ca. 20 km from the study area (Source: https://www.ilmatieteenlaitos.fi/havaintojen-lataus#!/).

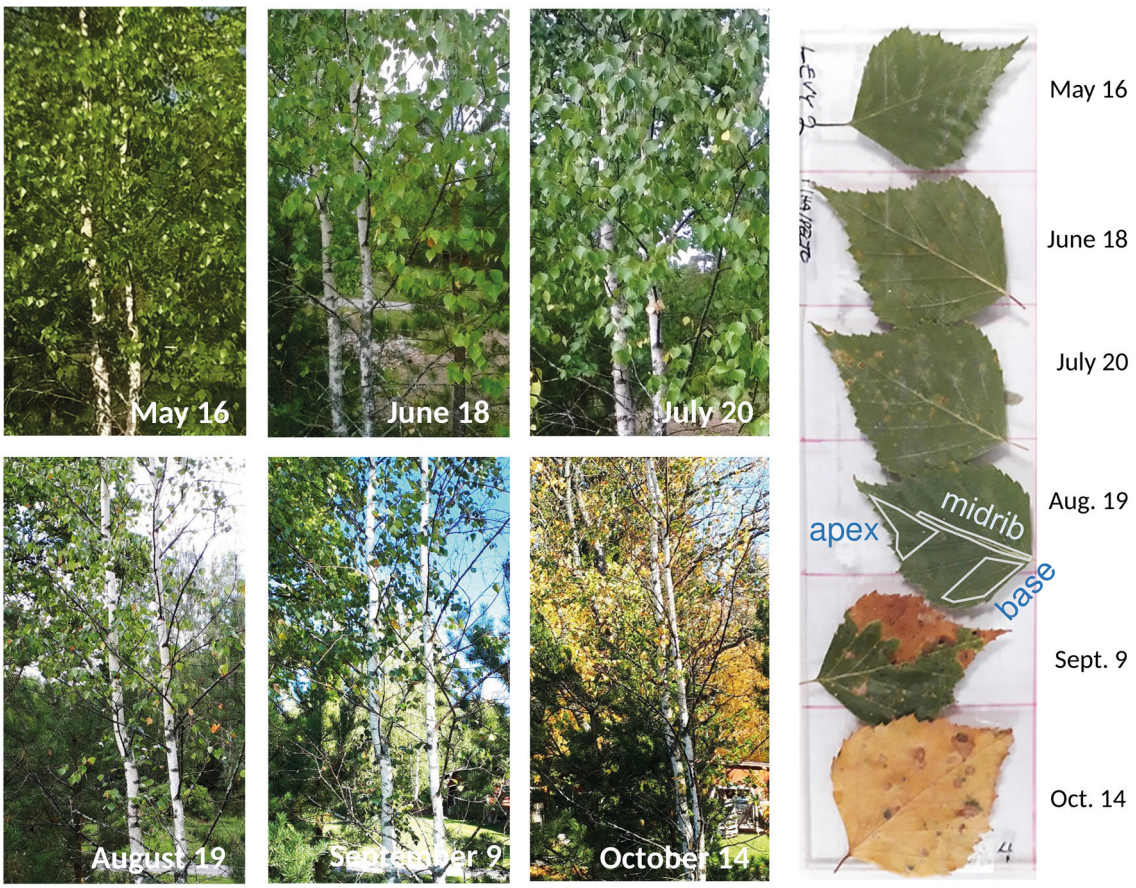

Fig. 2. Seasonal development of a sampled silver birch (tree number 4) in the rural habitat. On the right, consecutive leaf samples of the same tree when attached to a plexiglass plate. On the leaf collected on August 19, locations of the three digitised leaf areas are also shown.

We started our monthly tree sampling in May around one week after bud opening, and the last sampling was made six months later in October when the autumn leaves started to blow off in the wind (Fig. 2). Collections of three nearby trees in each habitat were made on the same days of the month. We pressed and dried samples of small branches from a height of around 160–200 centimetres. One tree in both the seashore and limestone habitats grew more isolated from the rest (Fig. 1). The sampled trees were 3 to 5 meters tall, with exception of 10 to 15 meters tall trees in rural (tree number 6), seashore (trees 7–9) and limestone (tree 18) habitats. Two road margin trees (numbers 10 and 12) were replaced with nearby trees from July onward because road maintenance cut down the original trees in late June. In the seepwater forest, birches showed also characteristics of *B. pubescens*.

After the field season, we selected a healthy-looking leaf from each collection and attached it to a plexiglass plate with double-sided adhesive tape. Each plate included 18 leaves from the same habitat. We mapped their element distributions in units of counts per second per electronvolt (cps/eV), which is relative to the abundance of an element in an object. The information depth or response depth of emergent X-ray radiation from the sample is closely linked to the atomic number of fluorescing element and composition of matrix (for details, see Haschke 2014; Flude et al. 2017). We hereafter apply the terms "content" or "level" when referring to these measurements. We applied the M4 Tornado micro-XRF spectrometer with an Rh anode in the Geoscientific Laboratory of the University of Turku. We focused the spot size of an X-ray beam with a polycapillary lens to about 20 μm and used the maximum of 50 kV voltage and 600 μA current. The total resolution of the measurement of a plate with 12 leaves was about 3800 rows and 2200 columns (ca. 4.4 million

pixels). A medium-sized leaf consisted of approximately 200 000 data points. We recorded the X-ray energy spectrums by using two silicon drift detectors calibrated with the zircon (Zr) standard before each sample plate measurement. The chamber pressure was set to 20 mbar, which allows for identifying most elements between sodium and uranium, but excluded some plant nutrients like boron and nitrogen from this study. After the raw data examination, we selected ten nutrient elements with measureable contents in all samples for the later phases of the analyses: Mg, Al, Si, P, S, K, Ca, Mn, Fe and Zn.

We produced 2D maps of each element using 50 µm steps and 5 ms dwelling times, and saved the data in hypermap files containing the full spectrum for each pixel. We normalised the colour intensities of the element maps to their highest values and applied deconvoluted counts. We digitised three different objects in each leaf, hereafter denominated as leaf areas (Fig. 2). MIDRIB was chosen because it is the primary vein with vascular bundles and also provides support for the entire leaf. The digitised area was a narrow belt starting from the junction of the petiole and leaf blade and extended to about two-thirds of the midrib length. LEAF BASE represents the major surface of leaf lamina with active photosynthesis; its delineation was made in either side of the midrib, excluding the outermost leaf margin yet including some side nerves. LEAF APEX is the distal part of the leaf blade with thin veins and probably low amounts of transient chemicals; the delineation was also done in either side of the midrib. Depending on the leaf sizes studied, the numbers of digitised pixels within individual polygons varied between 4109 (midrib in the smallest leaf) and 66 904 (leaf base of the biggest leaf). We recorded the average of pixel values of each polygon for the later analyses. We compiled the measurement data into a spreadsheet containing the monthly element measurements of six different habitats, each with the abovementioned leaf areas, the entire dataset thereby containing 108 data rows with 19 columns (Supplementary file S1, available at https://doi.org/10.14214/sf.10444).

We used SPSS Statistics for Windows (IBM Corp. 2017) in the statistical analyses. We first assessed the normality of the variable distributions visually, and then tested that with the Shapiro-Wilk test. In case of ANOVA and repeated measures ANOVA, normality checks were also carried out on the standardized residuals. Since the normality assumption was often inappropriate, non-parametric statistics were mainly used. We used scatter plots to visualise the two-dimensional distributions of different element pair combinations with their covariances tested with Spearman's rank correlation as a measure of the strengths and directions of their monotonic associations. Statistical differences in the monthly element contents ($n = 18$, i.e., six leaves every month, each with measurements from the midrib, base and apex) were tested with repeated measures ANOVA (rANOVA) with the Greenhouse-Geisser correction (only Mg), or in cases of non-normal distributions (other elements), we used the Friedman test with the post hoc Dunn-Bonferroni tests for their pairwise monthly comparisons.

Seasonal developments in the different habitats are visualised as line charts based on the mean values ($n = 9$, i.e., three sampled leaves with three measurements from each habitat). Statistical differences in the element contents between the different habitats were tested by using the Kruskal-Wallis test with post hoc Dunn-Bonferroni adjustment for their pairwise comparisons. Element contents in the different leaf areas (midrib, base and apex) were compared using line charts showing their monthly mean values ($n = 6$, i.e., six leaves each month). We tested statistical differences between the different leaf areas using the Kruskal-Wallis test with post hoc Dunn-Bonferroni adjustment for their pairwise comparisons.

We visually examined the element content maps to distinguish their detailed scaled foliar variations during the season and within individual leaves. Visual inspection required contrast enhancement, which was performed separately for each image. All the six monthly collected leaves from the same trees received the same treatment.

3 Results

Pairwise scatter plots suggest mainly weak associations between the contents of different foliar elements (Fig. 3). Statistically significant correlations occurred between Si and Al (Spearman's correlation coefficient 0.871, $p<0.001$), Fe and Al (0.725, $p<0.001$) and Fe and Si (0.809, $p<0.001$). Element maps of the example leaf (Fig. 3) shows the highest contents of the same elements and also Mn forming distinct accumulations in leaf blade margin and apex. Other statistically strong correlations ($p<0.001$) included nine positive and ten negative element pairs. However, their correlation coefficients were low, and their respective scatter plots did not suggest trend-like relationships. Some plots rather showed low values in either element to correspond with a broad range of values in the other. Examples of these include Mn with Al, Si and P.

All the studied elements showed statistically significant ($p<0.05$) differences between their monthly average levels (Fig. 4). Yet, the numbers of significantly dissimilar month-pairs varied between one (Mg, Zn) and eleven (S, K). Of the ten elements studied, seven showed statistically significant differences between May and June. Later in the season, dissimilarities between consecutive months were statistically significant in only a few cases: Mg (June vs. July), Al (August vs.

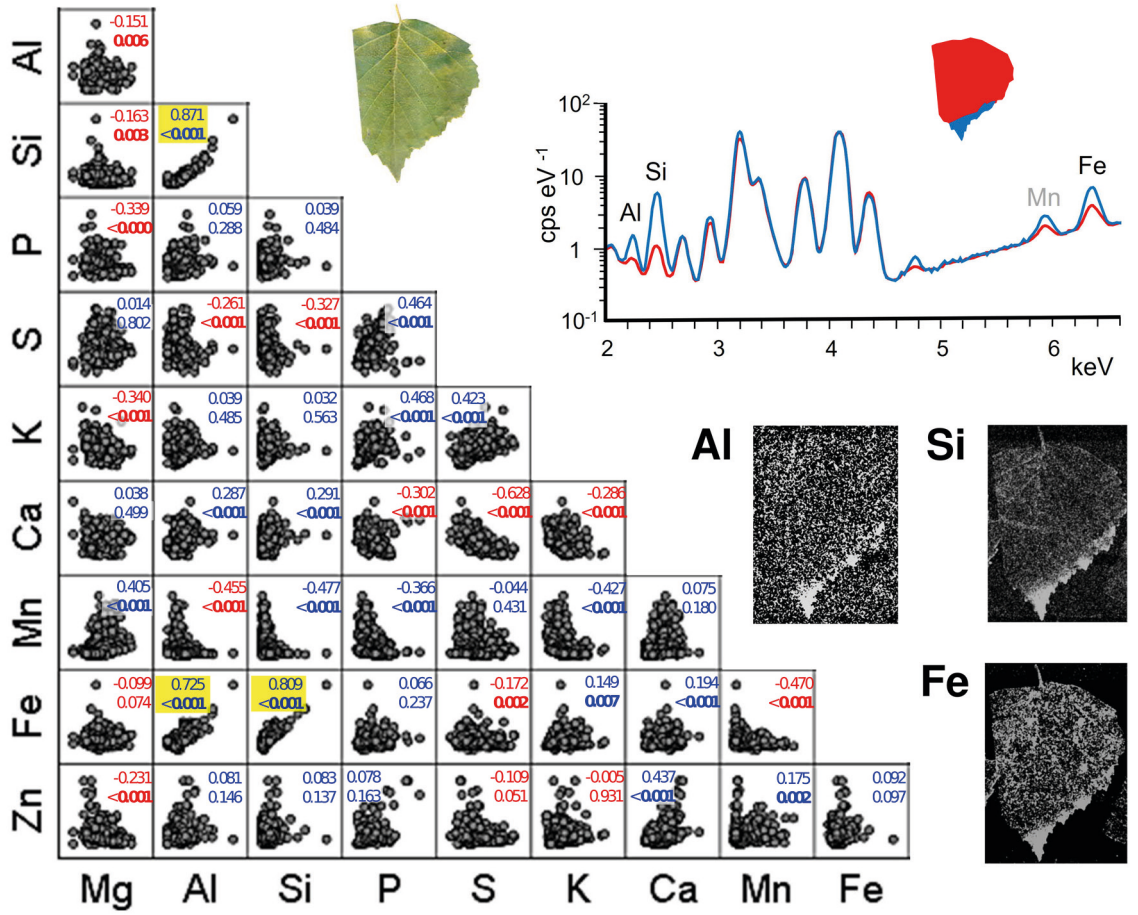

Fig. 3. Pairwise scatter plots with Spearman's correlation coefficients and p-values (bold: $p < 0.05$) between different pairs of foliar elements in the sampled silver birch trees. The points represent individual foliar measurements (n = 324, i.e. 6 habitats with 6 monthly collections of 3 leaves having 3 measured leaf parts). Positive correlations are indicated in blue, and negative are in red. Pairs with a strong positive trend ($p < 0.001$) are highlighted with yellow background. Right: An example leaf (roadmargin tree number 11 in September) in true colour, the XRF spectra for the red and blue leaf areas (selected element peaks are identified with labels), and the element maps of Al, Si and Fe.

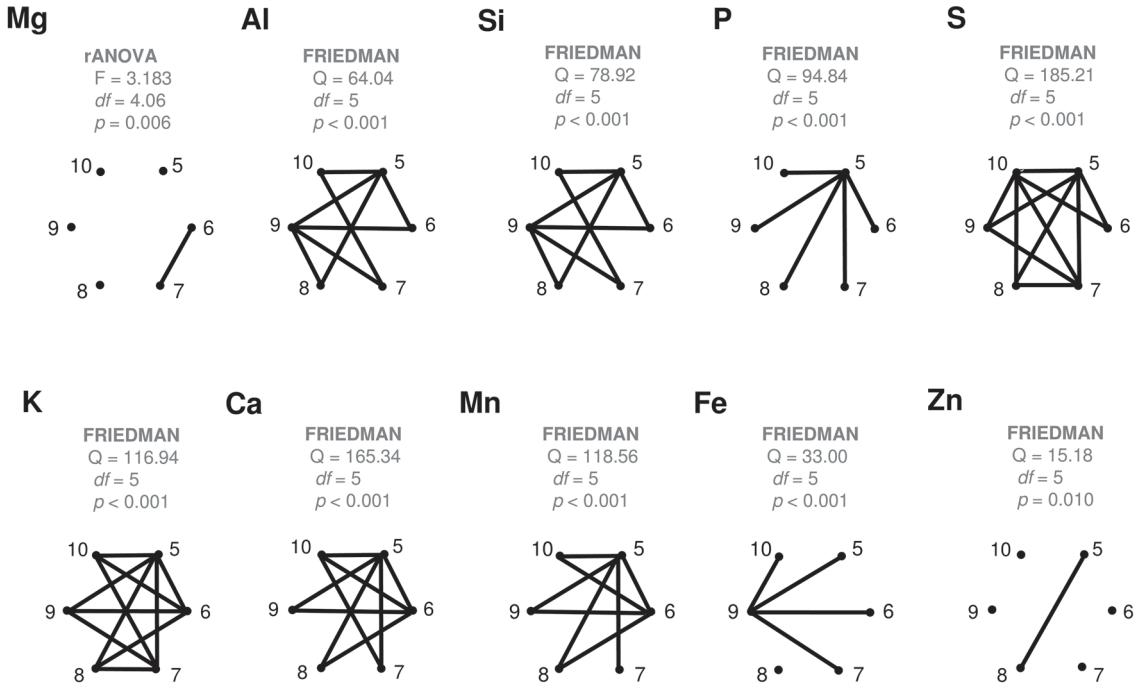

Fig. 4. Results of the statistical comparisons of the monthly contents of different elements in the collected silver birch leaves. Complete graphs show connecting edges between vertices (months) only when their difference is statistically significant ($p < 0.05$).

September), S (September vs. October), K (July vs. August), Si (August vs. September) and Fe (September vs. October). Zn did not have any succeeding month-pair with statistically significant differences. May values in P were statistically different from all the other months in the growing season. The September Fe levels were statistically different from all the other months except August.

Monthly element contents and their seasonal changes were dissimilar between the different habitats (Fig. 5). The contents of P, S and K decreased in most habitats as the season advanced with their steepest drops appearing most often between May and June. The opposite development with seasonally increasing levels occurred in Ca in all habitats, and in Mn and Zn in some habitats. The contents of Mg, Al, Si and Fe were variable between succeeding months in the road margin, seepwater and limestone habitats, yet they were stable in the other habitats. Limestone was the most distinctive of all habitats, having unique values or developments in all elements but S and K. However, each of the other habitats also revealed some uniqueness in one or two elements.

All elements but P showed dissimilarities between the different leaf areas (Fig. 6). The midrib differed significantly ($p < 0.05$) from other leaf areas by its elevated levels of Si, K, Ca, Zn, and to a degree also in Al and Fe. The opposite case with the lowest contents in the midrib occurred in Mg and S. Mn was the only element with statistically significant difference between the leaf apex with its elevated contents compared to the other leaf areas. In a more detailed examination of element distributions in micro-XRF maps (Fig. 7), Si, K, Ca, Zn (and more weakly, also Mn) showed elevated values in both the midrib and side veins. S was the only element showing lower content in the leaf veins than in the mesophyll. Especially K but also Mn and Zn showed variable element distributions at detailed scale between consecutive samples from the same trees. The high content areas of Si, Al, and Fe often formed distinct patches in leaf apex or margins (see also Fig. 3).

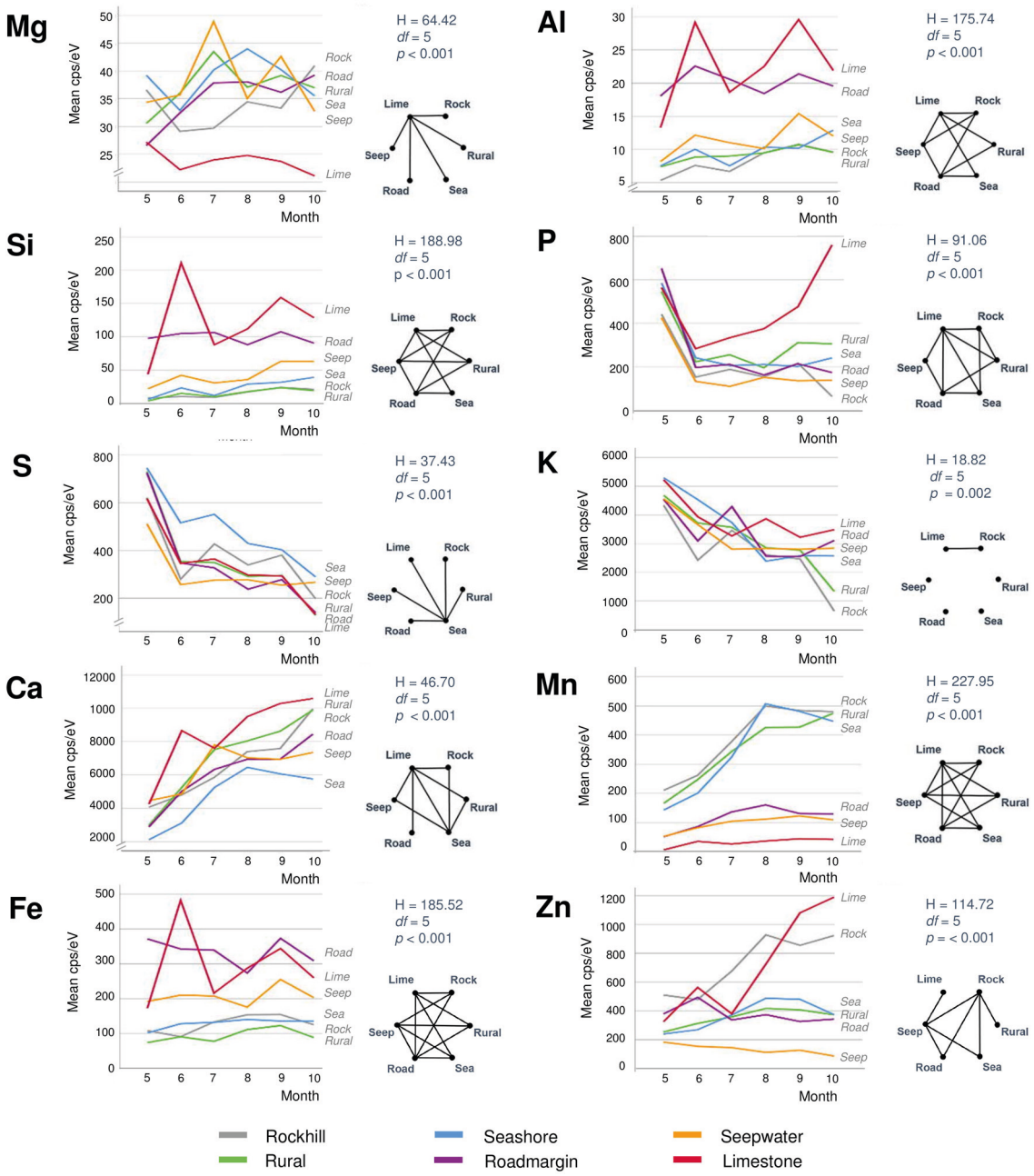

Fig. 5. Monthly average contents of ten different elements of silver birch leaves in six different habitats. The right-hand sides of each element show results from the Kruskal-Wallis tests (above) and pairwise Dunn-Bonferroni comparisons in the form of complete graphs showing connecting edges between vertices (habitats) only when their difference is statistically significant ($p < 0.05$).

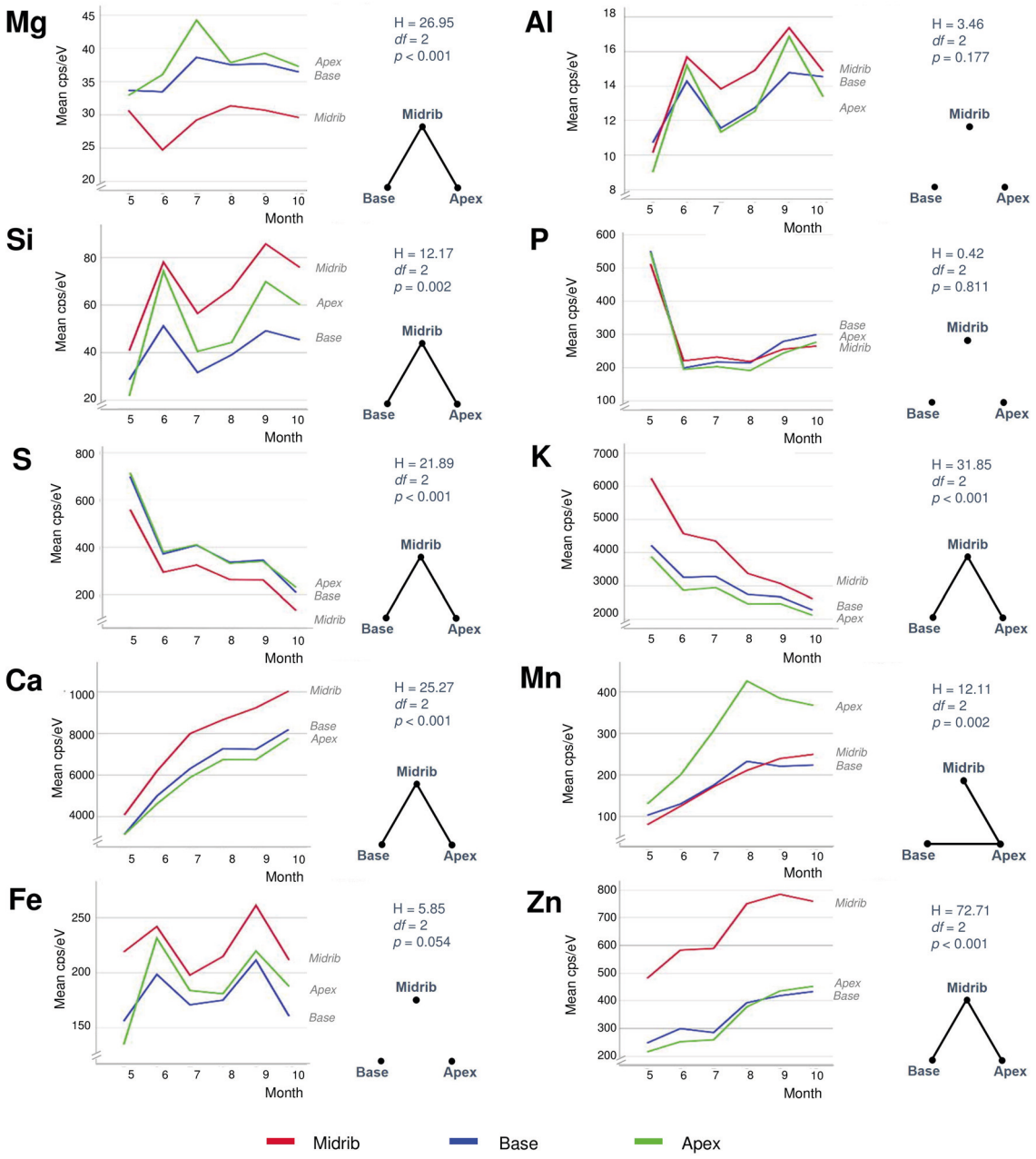

Fig. 6. Monthly average contents of ten different elements of silver birch leaves in three different leaf areas (see Fig. 2). The right-hand sides of each element show results from the Kruskal-Wallis tests (above) and pairwise Dunn-Bonferroni comparisons in the form of complete graphs showing connecting edges between vertices (habitats) only when their difference is statistically significant ($p < 0.05$).

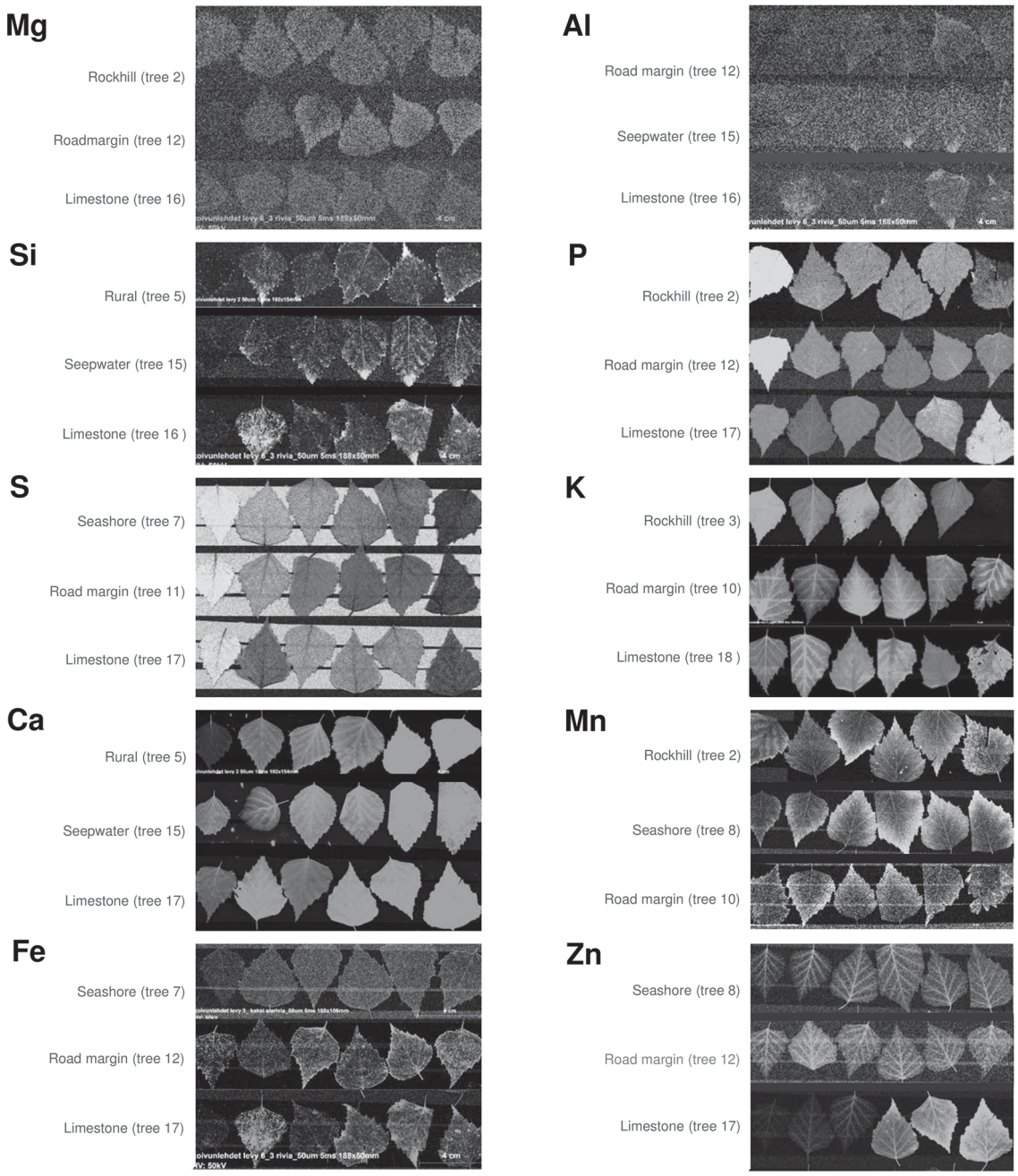

Fig. 7. Element maps by micro-XRF showing monthly collected silver birch leaves from May (left) to October (right). Each of the ten elements contains three time series as a selection of illustrative cases to compare with Figs. 5 and 6. Lighter colors indicate higher values but brightness variations are not linearly related to element contents.

4 Discussion

None of the ten studied elements was stable throughout the life cycle from young leaves to leaf senescence (Table 1). In many elements, either the youngest or the oldest leaves showed particularly high or low levels compared with the middle growing season (Fig. 5). Only Fe had almost the same contents in the beginning and end of the season. Although nutrient levels in May were often close to each other in different habitats (not Mg, Al, Fe and Mn), their later developments showed disparate characteristics. Such variations probably reflect permanent site properties (Fontana et al. 2018) by

Table 1. Summary of the main findings regarding the seasonal, between-habitat and leaf level variations of silver birch leaves for the ten studied elements.

Element	Seasonal change	Differences between habitats	Differences between leaf areas	Remarks
Mg	Barely any trend	Low in limestone	Low in midrib	Distinct in June
Al	Barely any trend	High in limestone and road margin	Elevated in midrib	Correlations with Si and Fe
Si	Barely any trend	High in limestone and road margin	High in midrib	Correlations with Al, Fe
P	High in May	Late summer increase in limestone	No differences	Decrease from May to June
S	Strong decrease	High in seashore	Low in midrib	Low before abscission
K	Decrease	Dissimilar contents in October	High in midrib	Variable XRF maps
Ca	Strong increase	Limestone the highest, seashore the lowest	High in midrib	Moist habitats exceptional
Mn	Local increases	Habitats appear in two groups	High in apex	High contents at leaf margins
Fe	Sometimes two peaks	High in road margin and limestone	Possibly elevated in midrib	Correlations with Al and Si
Zn	Increase	Late summer high in limestone and rockhill	Very high in midrib	Low levels in seepwater

factors like parent material chemistry, the weathering of minerals, soil formation, microclimate, soil water retention capacity and soil metabolic activity (Neff et al. 2006; Heiskanen et al. 2018).

Foliar magnesium varied locally without consistent change pattern. Mg is a comparatively mobile macronutrient with its availability to plants depending on many different factors from the source rock material to climate and soils (Gransee and Führs 2013). The remarkably low foliar Mg in the limestone habitat could reflect the antagonistic effect of high availability of Ca to Mg uptake. Lacking correlation between these elements in our full data (Fig. 3) is not necessarily contradictory to this notion because lower Ca levels can, in turn, be positively synergistic with Mg uptake (Gransee and Führs 2013). At the scale of leaf, the lowest Mg contents occur in the midrib (Fig. 6) but this characteristic is difficult to depict from the element maps which suffer from ample noise (Fig. 7).

Phosphorous peaked in the expanding leaves in May (Figs. 4 and 5). In the full-sized leaves in June, P contents were lower and showed only small changes during the later season. These results are in line with previous studies of P dynamics in *Betula* foliage (Tamm 1951; Ferm and Markkola 1985; Chapin III and Kedrowski 1983). However, the limestone habitat was exceptional by showing increasing P content after June. Although the local marble-like limestone does not include P, calcareous dust precipitation from the nearby quarry could increase soil pH after winter. It is generally considered that the maximum P availability to plants occurs at near-neutral pH conditions (Penn and Camberato 2019). It would be interesting to monitor soil pH changes in the limestone habitat from spring to fall.

Foliar sulphur declined in all trees as the season advanced (Fig. 5). S contents were the highest in May when this nutrient is needed to synthesise proteins, lipids and defence substances (Hartmann et al. 2000). Later during the growing season, S contents declined, reaching their lowest levels in October. Comparing different habitats, S contents were high at the seashore as a likely consequence of direct root contact with seawater sulphates in soil solute. In the leaves, S contents were the lowest in the midrib area (Fig. 6) and side veins (Fig. 7). According to Takahashi (2019), sulphate ions translocated form the shoot unload from the xylem through ion leakage and distribute from veins in the integral photosynthetic leaf tissues.

Also foliar potassium was high in May, after which its contents decreased (Fig. 5). The decrease was particularly steep in the rockhill and rural habitats just before the leaf fall. In the

other habitats, late season K contents were moderately variable. Foliar K contents were remarkably high in the midrib and side veins (Figs. 6 and 7), yet also the opposite situation was found in individual leaf samples (tree 18 in August). The micro-XRF maps also reveal some unusual patterns of K distributions near the boundaries between the vascular bundles and mesophyll. These findings draw attention to the highly mobile traits of K^+ nutrition in plants where it is needed for a number of vital processes from photosynthesis to the regulation of stomata (Ragel et al. 2019).

Calcium generally increased with the advancing season (Fig. 5). Unlike the downy birches studied by Ferm and Markkola (1985), none of our trees showed high foliar Ca in May. Leaves collected from the limestone habitat had the highest Ca levels. In the seashore and to some degree also seepwater, Ca decreased after midsummer. Abundant soil water may decrease Ca availability to plants but alternative explanations might be sought from tree physiology under water stress. Ca levels were the highest in the midrib and side veins (Figs. 6 and 7), which are the strongest parts of leaf. Foliar calcification has the function to support membrane stability and cell wall lignification in senescing leaves (Santa Regina et al. 1997; Hawkesford et al. 2012).

Manganese increased in three adjacent habitats (rockhill, rural, seashore) with the advancing season (Fig. 5). A possible explanation is the local geology since in a bedrock well of the same area, high Mn levels have been detected (250 µg dm^{-3}; RK, unpublished information). In the rest of habitats, Mn levels did not change much. The detailed patterns of foliar Mn distributions were intriguing with its high values at the leaf blade margins including apex (Figs. 6 and 7). We have not found descriptions of similar Mn distributions in earlier studies but hypothesise the following: As excess amounts Mn can become toxic and plants have evolved mechanisms to regulate its uptake, trafficking, and storage (Broadley et al. 2012; Alejandro et al. 2020), birches may sequester excessive Mn at their leaf margins.

Zinc displayed various types of seasonal developments. The only month pair with statistically significant difference was May with August (Fig. 4). Instead, the most distinctive dissimilarities occurred between habitats (Fig. 5): Zn was low and decreasing in one habitat (seepwater), showed a shallow peak in late summer (seashore, rural, roadmargin) or presented strong increase toward the late growing season (rockhill, limestone). On the rockhill, Zn accumulation may reflect local geology and pH, but in the limestone habitat also an anthropogenic factor must also be considered since the sampled trees grew close to a galvanised steel fence. Because the major determining factor affecting Zn solubility in soil solution is pH (Gupta et al. 2016), future studies should address this parameter. In the leaves, Zn contents were elevated in the foliar veins (Figs. 6 and 7). However, some leaves had high Zn contents also in the leaf blade margins suggesting sequestration of its excess amounts (e.g., tree number 17 in the limestone habitat, Fig 7).

The remaining elements of aluminium, silica and iron were strongly correlated: Their highest levels occurred in the same months (June, September), habitats (limestone, road margin) and parts of leaves (midrib, accretions at leaf margins). This is interesting, since the functions of these elements are highly dissimilar in plant physiology. Al is not needed but it can be toxic (Foy et al. 1978). Si is nonessential, yet it supports plant life, structure and resistance to stress (Epstein 2009). Fe is an essential micronutrient contributing to the formation of chlorophyll and diverse enzyme systems – although becomes toxic when excessive (Foy et al. 1978; Briat et al. 2015). We infer that the strong association of these elements in our data emphasises the role of Si in alleviating the metallic toxicities of Al and Fe (Ma 2005). Tolra et al. (2011) similarly suggested that Si might contribute to the internal detoxification of Al in *Faramea marginata* Cham. Additionally, elevated Si contents also occurred in leaf veins and the tips of leaf margin teeth (Fig. 7). In these parts of leaf, Si probably contributes to structural rigidity.

The broad results of this study can be summarised as follows. Seasonal changes in the essential macronutrients (except Mg) were rather even between the different habitats, but their detailed

distributions at the leaf-scale were variable. Micronutrients (Fe, Mn, Zn) and non-essential elements (Al, Si) showed more conspicuous differences between habitats, and they likewise exposed fine-scaled nuances in their distributions within the leaf blades. The limestone habitat had distinctive foliar contents or developments in almost all elements but S and K (Fig. 5). Other habitats with unique levels of some elements included seashore (S, Ca) and seepwater (Zn). Because our study year was particularly dry, we also had a possibility to see changes caused by drought stress. Although we avoided collecting injured leaves, three leaf samples nevertheless included partial drought-induced yellowing or browning, each with lowered levels of the macronutrients P, S and K (Fig. 8). None of the other elements showed similar changes. It thereby seems that birches translocate these macronutrients before permanent leaf scorches form.

Element mapping by micro-XRF is an agile and cost-efficient way to study field samples with low need for sample preparation. However, its methodological restrictions must also be understood. For example the maximum response depth of metals in biological samples varies in the order of hundreds of micrometers according element atomic numbers (Perez et al. 2010; Haschke 2014). Accordingly, the measured metal contents by micro-XRF may not always represent the entire leaf thickness or part of information includes signal from also behind the leaves (adhesive tape, plexiglass; see the maps of S, K, Fe, Mn and Zn (Fig. 7). The visual interpretation of strongly enhanced element maps (Figs. 7 and 8) must also be made with care since their brightness variations are not linearly related to element contents. Further, the maps of light elements with low signal-to-noise ratio (Mg, Al) suffer from noisiness. These conditions understood, element mapping by micro-XRF provides intriguing possibilities to study plant responses to their environment with high structural detail. When elements should be quantified according to their foliar concentrations (solute relative to mass or volume) instead of the scale of cps/eV, empirical testing is needed to establish their relations.

Silver birch commonly grows best in well-drained fertile sandy soils (Hynynen et al. 2010). As a common successional tree it also abounds in many suboptimal environments, such as the

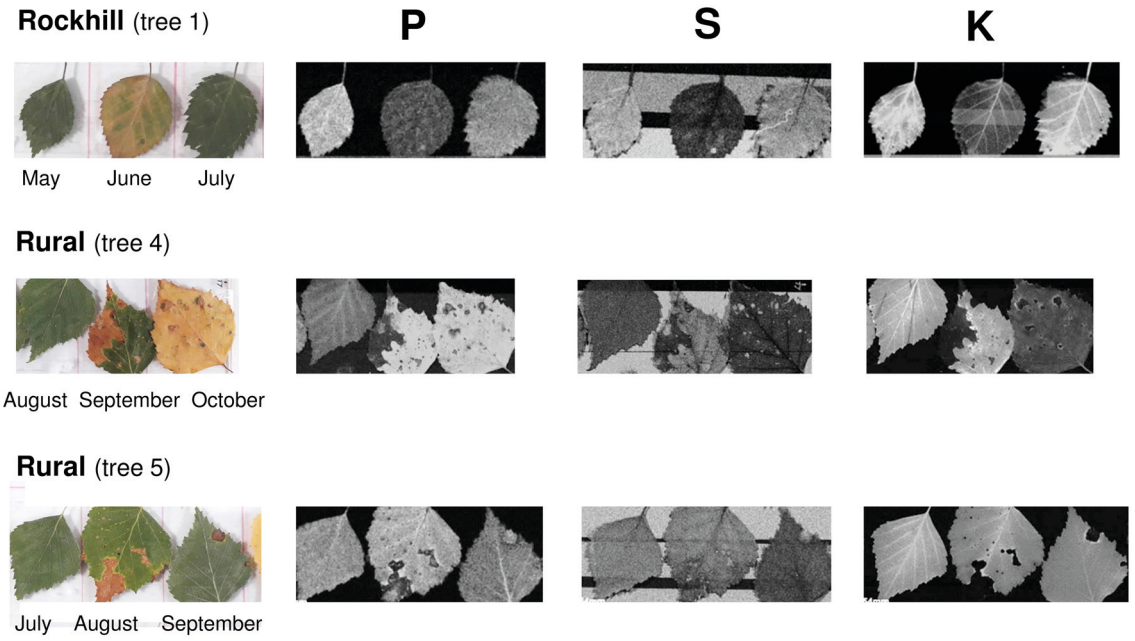

Fig. 8. Partial leaf browning or yellowing in silver birch leaves due to drought-induced problems in three study trees. In the series of three consecutive months, the samples with drought symptoms are in the middle. Lighter colors indicate higher values but brightness variations are not linearly related to element contents.

rockhill and seashore habitats of this study. When nearby habitats occur as a dense mosaic, the stands of this wind-dispersed and wind-pollinated species are from the same gene pool. We thereby infer that the here documented foliar element dynamics confirm the physiological plasticity of this species to cope with local and temporal environmental variabilities. Future investigations in combination with soil studies can establish more precise traits between the foliar nutrients, their roles in plant functional physiology and interactions with the environment.

Acknowledgments

We thank Dr. Kalle Ruokolainen for insightful discussions during the planning of this research idea, and Dr. Timo Kilpeläinen for his shared knowledge about the local geology.

Supplementary files

S1.pdf, available at https://doi.org/10.14214/sf.10444.

References

Alejandro S, Höller S, Meier B, Peiter E (2020) Manganese in plants: from acquisition to subcellular allocation. Front Plant Sci 11, article id 300. https://doi.org/10.3389/fpls.2020.00300.

Briat JF, Dubos C, Gaymard F (2015) Iron nutrition, biomass production, and plant product quality. Trends Plant Sci 20: 33–40. https://doi.org/10.1016/j.tplants.2014.07.005.

Broadley M, Brown P, Cakmak I, Rengel Z, Zhao F (2012) Functions of nutrients: micronutrients. In: Marschner P (ed) Marschner's mineral nutrition of higher plants. Academic Press, pp 191–248. https://doi.org/10.1016/B978-0-12-384905-2.00007-8.

Chabot BF, Hicks DJ (1982) The ecology of leaf life spans. Annu Rev Ecol Syst 13: 229–259. https://doi.org/10.1146/annurev.es.13.110182.001305.

Chapin III FS, Kedrowski RA (1983) Seasonal changes in nitrogen and phosphorus fractions and autumn retranslocation in evergreen and deciduous taiga trees. Ecology 64: 376–391. https://doi.org/10.2307/1937083.

Epstein E (2009) Silicon: its manifold roles in plants. Ann Appl Biol 155: 155–160. https://doi.org/10.1111/j.1744-7348.2009.00343.x.

Ferm A, Markkola A (1985) Hieskoivun lehtien, oksien ja silmujen ravinnepitoisuuksien kasvukautinen vaihtelu. [Nutritional variation of leaves, twigs and buds in *Betula pubescens* stands during the growing season]. Folia Forestalia 613. http://urn.fi/URN:ISBN:951-40-0689-5.

Fittschen UEA, Falkenberg G (2011) Trends in environmental science using microscopic X-ray fluorescence. Spectrochim Acta Part B At Spectrosc 66: 567–580. https://doi.org/10.1016/j.sab.2011.06.006.

Fittschen UEA., Kunz HH, Höhner R, Tyssebotn IMB, Fittschen A (2017) A new micro X-ray fluorescence spectrometer for in vivo elemental analysis in plants. X-Ray Spectrom 46: 374–381. https://doi.org/10.1002/xrs.2783.

Flude S, Haschke M, Storey M (2017) Application of benchtop micro-XRF to geological materials. Mineral Mag 81: 923–948. https://doi.org/10.1180/minmag.2016.080.150.

Fontana M, Labrecque M, Messier C, Bélanger N (2018) Permanent site characteristics exert a larger influence than atmospheric conditions on leaf mass, foliar nutrients and ultimately aboveground

biomass productivity of *Salix miyabeana* 'SX67'. For Ecol Manage 427: 423–433. https://doi.org/10.1016/j.foreco.2018.02.005.

Foy CD, Chaney RT, White MC (1978) The physiology of metal toxicity in plants. Annu Rev Plant Physiol 29: 511–566. https://doi.org/10.1146/annurev.pp.29.060178.002455.

Gransee A, Führs H (2013) Magnesium mobility in soils as a challenge for soil and plant analysis, magnesium fertilization and root uptake under adverse growth conditions. Plant Soil 368: 5–21. https://doi.org/10.1007/s11104-012-1567-y.

Gupta N, Ram H, Kumar B (2016) Mechanism of Zinc absorption in plants: uptake, transport, translocation and accumulation. Rev Environ Sci Biotechnol 15: 89–109. https://doi.org/10.1007/s11157-016-9390-1.

Gupta S, Rupasinghe T, Callahan DL, Natera SH, Smith PM, Hill CB, Roessner U, Boughton BA (2019) Spatio-temporal metabolite and elemental profiling of salt stressed barley seeds during initial stages of germination by MALDI-MSI and μ-XRF spectrometry. Front Plant Sci 10, article id 1139. https://doi.org/10.3389/fpls.2019.01139.

Hartmann T, Mult S, Suter M, Rennenberg H, Herschbach C (2000) Leaf age-dependent differences in sulphur assimilation and allocation in poplar (*Populus tremula*× *P. alba*) leaves. J Exp Bot 51: 1077–1088. https://doi.org/10.1093/jexbot/51.347.1077.

Haschke M (2014) Laboratory micro-X-ray fluorescence spectroscopy. Springer Ser Surf Sci 55, Springer, Cham. https://doi.org/10.1007/978-3-319-04864-2.

Hawkesford M, Horst W, Kichey T, Lambers H, Schoerring J, Skrumsager I, White P (2012) Functions of macronutrients. In: Marschner P (ed) Marschner's mineral nutrition of higher plants. Academic Press, pp 135–189. https://doi.org/10.1016/B978-0-12-384905-2.00006-6.

Heiskanen J, Hallikainen V, Uusitalo J, Ilvesniemi H (2018) Co-variation relations of physical soil properties and site characteristics of Finnish upland forests. Silva Fenn 52, article id 9948. https://doi.org/10.14214/sf.9948.

Helmisaari HS (1990) Temporal variation in nutrient concentrations of *Pinus sylvestris* needles. Scand J For Res 5: 177–193. https://doi.org/10.1080/02827589009382604.

Hynynen J, Niemistö P, Viherä-Aarnio A, Brunner A, Hein S, Velling P (2010). Silviculture of birch (*Betula pendula* Roth and *Betula pubescens* Ehrh.) in Northern Europe. Forestry 83: 103–119. https://doi.org/10.1093/forestry/cpp035.

IBM Corp. (2017) IBM SPSS statistics for Windows, version 25.0. IBM Corp., Armonk, NY.

Karhunen R (2004) Iniön ja Turun kartta-alueiden kallioperä. [Pre-Quaternary rocks of the Iniö and Turku map-sheet areas]. Geological map of Finland 1:100000. https://www.yumpu.com/fi/document/read/48619069/tassa-arkistogsffi-geologian-tutkimuskeskus. Accessed 25 November 2020.

Ma JF (2005) Plant root responses to three abundant soil minerals: silicon, aluminum and iron. Crit Rev Plant Sci 24: 267–281. https://doi.org/10.1080/07352680500196017.

Marschner P (2012) Marschner's mineral nutrition of higher plants. Third edition. ISBN 978-0-12-384905-2. Academic Press. https://www.sciencedirect.com/book/9780123849052/marschners-mineral-nutrition-of-higher-plants.

McHargue JS, Roy WR (1932) Mineral and nitrogen content of the leaves of some forest trees at different times in the growing season. Bot Gaz 94: 381–393. https://doi.org/10.1086/334303.

Messenger SA (1984) Seasonal variations of foliar nutrients in green and chlorotic red maples. J Environ Hortic 2: 117–119. https://doi.org/10.24266/0738-2898-2.4.117.

Mitchell HL (1936) Trends in the nitrogen, phosphorus, potassium and calcium content of the leaves of some forest trees during the growing season. Black Rock For Pap 1: 30–44. http://blackrockforest.org/files/blackrock/content/BRF%20PAPERS%20NO.6.pdf.

Neff JC, Reynolds R, Sanford RL, Fernandez D, Lamothe P (2006) Controls of bedrock geochem-

istry on soil and plant nutrients in southeastern Utah. Ecosystems 9: 879–893. https://doi.org/10.1007/s10021-005-0092-8.

Pavlović M, Rakić T, Pavlović D, Kostić O, Jarić S, Mataruga Z, Pavlović P, Mitrović M (2017) Seasonal variations of trace element contents in leaves and bark of horse chestnut (*Aesculus hippocastanum* L.) in urban and industrial regions in Serbia. Arch Biol Sci 69: 201–214. http://dx.doi.org/10.2298/ABS161202005P.

Peel MC, Finlayson BL, McMahon TA (2007) Updated world map of the Köppen-Geiger climate classification. Hydrol Earth Syst Sci 11: 1633–1644. https://doi.org/10.5194/hess-11-1633-2007.

Penn CJ, Camberato JJ (2019) A critical review on soil chemical processes that control how soil pH affects phosphorus availability to plants. Agriculture 9, article id 120. https://doi.org/10.3390/agriculture9060120.

Perez RD, Sánchez HJ, Perez CA, Rubio M (2010) Latest developments and opportunities for 3D analysis of biological samples by confocal μ-XRF. Radiat Phys Chem 79: 195–200. https://doi.org/10.1016/j.radphyschem.2009.04.034.

Ragel P, Raddatz N, Leidi EO, Quintero FJ, Pardo JM (2019) Regulation of K+ nutrition in plants. Front Plant Sci 10, article id 281. https://doi.org/10.3389/fpls.2019.00281.

Santa Regina I, Rico M, Rapp M, Gallego HA (1997) Seasonal variation in nutrient concentration in leaves and branches of *Quercus pyrenaica*. J Veg Sci 8: 651–654. https://doi.org/10.2307/3237369.

Suominen T, Tolvanen H, Kalliola R (2010) Surface layer salinity gradients and flow patterns in the archipelago coast of SW Finland, northern Baltic Sea. Mar Environ Res 69: 216–226. https://doi.org/10.1016/j.marenvres.2009.10.009.

Takahashi H (2019) Sulfate transport systems in plants: functional diversity and molecular mechanisms underlying regulatory coordination. J Exp Bot 70: 4075–4087. https://doi.org/10.1093/jxb/erz132.

Tamm CO (1951) Seasonal variation in composition of birch leaves. Physiol Plant 4: 461–469. https://doi.org/10.1111/j.1399-3054.1951.tb07683.x.

Tian S, Lu L, Xie R, Zhang M, Jernstedt J, Hou D, Ramsier C, Brown P (2015) Supplemental macronutrients and microbial fermentation products improve the uptake and transport of foliar applied zinc in sunflower (*Helianthus annuus* L.) plants. Studies utilizing micro X-ray florescence. Front Plant Sci 5, article id 808. https://doi.org/10.3389/fpls.2014.00808.

Tolra R, Vogel-Mikuš K, Hajiboland R, Kump P, Pongrac P, Kaulich B, Gianoncelli A, Babin V, Barceló J, Regvar M, Poschenrieder C (2011) Localization of aluminium in tea (*Camellia sinensis*) leaves using low energy X-ray fluorescence spectro-microscopy. J Plant Res 124: 165–172. https://doi.org/10.1007/s10265-010-0344-3.

Voegelin A, Weber FA, Kretzschmar R (2007) Distribution and speciation of arsenic around roots in a contaminated riparian floodplain soil: micro-XRF element mapping and EXAFS spectroscopy. Geochim Cosmochim Acta 71: 5804–5820. https://doi.org/10.1016/j.gca.2007.05.030.

Total of 41 references.